

2

Polarized site-selected fluorescence spectroscopy of isolated Photosystem I particles

Bas Gobets, Herbert van Amerongen, René Monshouwer, Jochen Kruij, Matthias Rögner, Rienk van Grondelle and Jan P. Dekker

Polarized steady-state fluorescence spectra have been obtained from Photosystem I core complexes of the cyanobacterium *Synechocystis* PCC 6803 and from LHCI containing Photosystem I (PSI-200) complexes of spinach by selective laser excitation at 4 K. Excitation above 702 nm in *Synechocystis* and 720 nm in PSI-200 results in highly polarized emission, suggesting that pigments absorbing at these and longer wavelengths are not able to transfer excitation energy at 4 K. In both systems the peak wavelength of the emission (λ_{em}) depends strongly on the excitation wavelength (λ_{ex}). This indicates that in both systems the long-wavelength bands responsible for the steady-state emission are inhomogeneously broadened. The width of the inhomogeneous distribution is estimated to be about 215 cm^{-1} in *Synechocystis* and 400 cm^{-1} in PSI-200. We conclude that the peaks of the total absorption spectra of the long-wavelength pigments of *Synechocystis* and PSI-200 are at 708 and 716 nm, respectively, and therefore designate these pigments as C708 and C716. The results further show that C708 and C716 are strongly homogeneously broadened, i.e. carry broad phonon side-bands. The width of these bands is estimated to be about 170 and 200 cm^{-1} for C708 and C716, respectively. The Stokes' shifts appear to be large: about 200 cm^{-1} (10 nm) for C708 and about 325 cm^{-1} (17 nm) for C716. These values are much higher than usually observed for 'normal' antenna pigments, but are in the same order as found previously for a number of dimeric systems. Therefore, we propose that the long-wavelength pigments in Photosystem I are excitonically coupled dimers. Based on fitting with Gaussian bands the presence of one C708 dimer per P700 is suggested in the core antenna of *Synechocystis*.

INTRODUCTION

The two main functions of the light-harvesting antenna pigments in photosynthetic systems are the absorption of light of different wavelengths and the efficient transfer of excitation energy to one of the photochemical reaction centres. Both functions are highly optimized in photosynthetic organisms: the antenna usually absorbs as much as possible of the available light, and excitation energy transfer to the reaction centre is generally highly efficient.¹

In Photosystem I (PSI) of green plants, algae and cyanobacteria it has been shown that excitation energy transfer is indeed extremely rapid.² The most recent experiments suggest average single transfer times of about 180 fs³ and overall trapping times in the tens of picoseconds time-range.⁴⁻⁶ According to Trissl^{6,7} these processes in PSI are even more efficient than actually required, due to which the photosystem can afford a small number of antenna pigments absorbing at lower energy than the primary electron donor P700, thus increasing the absorption cross-section for red light (> 700 nm) and optimizing the balance between the two main functions. In addition, some of the long-wavelength pigments could help in guiding the excitations to P700.^{4,8} The long-wavelength pigments largely determine the steady-state emission properties at low temperatures. Such pigments in most of the PSI reaction centre core complexes of green plants, algae and cyanobacteria give rise to emission bands peaking near 720 nm at 77K, while most of the peripheral chlorophyll-*a/b* antenna complexes give rise to emission bands peaking near 735 nm.⁹

Despite substantial interest in the role of long-wavelength pigments of PSI in excitation energy transfer and trapping, there is still considerable lack of knowledge about their molecular properties. The number of red pigments per complex, the exact absorption maxima, the extent of homogeneous and inhomogeneous broadening and the possibility of energy transfer between the red pigments are, for instance, not well known. In a previous report, we analysed a number of isolated PSI preparations (monomeric and trimeric core complexes from the cyanobacterium *Synechocystis* PCC 6803 and LHCI containing PSI-200 complexes from spinach) by steady-state polarized light spectroscopy at 77 K and linear and circular dichroism characteristics were established.¹⁰ It was concluded that the possibility of energy transfer between the various long-wavelength pigments was very low in the monomeric and trimeric particles from *Synechocystis*, but high in PSI-200, in which significant downhill energy-transfer from the long-wavelength pigments of the core antenna to the peripheral antenna was proposed.

In this report, we extend this research by polarized site-selected fluorescence spectroscopy, provide new information on the spectroscopic properties of the long-wavelength pigments in the core and peripheral antenna of PSI, and propose that these pigments are arranged as excitonically coupled dimers of chl*a*.

MATERIALS AND METHODS

Monomeric and trimeric PSI core particles (P700-F_A/F_B) from *Synechocystis* sp. PCC 6803 were prepared as described before by Rögner and co-workers.^{11,12} Unlike the complexes studied in ref. 10, the absorption profiles at long wavelengths were similar for the monomeric

and trimeric complexes and the membranes studied in this contribution (see Section 3). For a possible explanation we suggested that the amplitude of the long-wavelength spectral component in the monomers varies per batch and depends on the severeness of the detergent treatment during the isolation procedure.¹⁰ Obviously, the monomeric complexes analysed in this contribution are more native. LHCl containing PSI-200 particles from spinach were prepared as described by Van der Lee et al.¹⁰ For the low-temperature measurements, the particles were diluted in 20 mM Mes-NaOH, 10 mM MgCl₂, 10 mM CaCl₂, 70% w/v glycerol and 0.05% dodecyl- β ,D-maltoside (pH 6.5) and cooled to 4 K in a He-flow cryostat (Oxford).

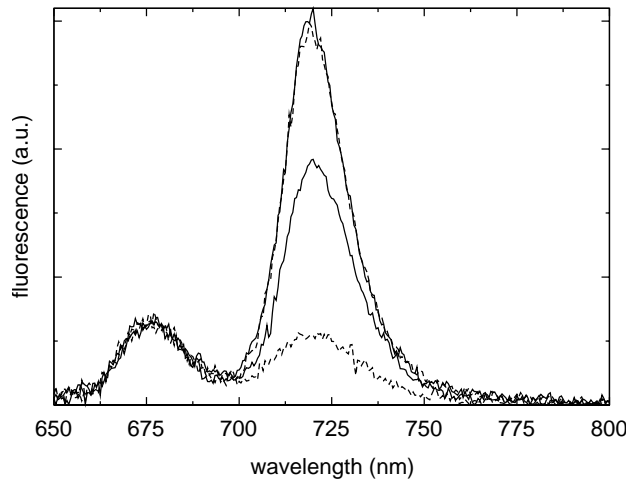
Fluorescence spectra were obtained on a home-built fluorimeter and corrected for the sensitivity of the detection system as in ref. 13. Site-selection was performed as in ref. 14, except that as light source for the site-selection excitation light a Ti-Sapphire laser was used (Coherent, model 890, spectral bandwidth $\sim 2 \text{ cm}^{-1}$). The laser was tuned between 693.5 and 733.5 nm at 1 nm intervals, using 4–20 mW/cm² energy. It was checked that no sample degradation took place during the measurements. Detection of the fluorescence was at right angle with respect to the excitation beam and was achieved with a double 1/8 m monochromator (Oriel) and a photomultiplier (S-20 photocathode, Thorn EMI 9658A). The spectral bandwidth for detection was 1.5 nm. The excitation light was vertically polarized (when sensitivity corrections were made horizontally polarized excitation was used as well) and a polarizer in the detection beam was either vertical or horizontal. The anisotropy of the emission is defined by $r = (I_{||} - I_{\perp}) / (I_{||} + 2I_{\perp})$, in which $I_{||}$ and I_{\perp} are the fluorescence intensities with vertical and horizontal detection beam polarizations, respectively. The site-selected spectra were recorded with $A_{680} \sim 1$. This high A was used to increase the fluorescence intensity. Self-absorption of the emitted light did not pose a serious problem, because the fluorescence appeared far away from the maximum of the absorption. Absorption spectra were measured on a Cary 219 spectrophotometer with 0.25 nm resolution.

RESULTS

Photosystem I core complexes from *Synechocystis*

Cyanobacteria like *Synechocystis* contain reaction centre core complexes of PSI, but lack peripheral chl*a/b* containing antenna complexes. Isolated cyanobacterial cores, including those of *Synechocystis*, have been isolated as monomeric and/or as trimeric complexes.^{15,18} There is increasing evidence that the trimeric association represents the *in vivo* organization of the cyanobacterial core under certain salt conditions,^{16–18} presumably in equilibrium with the monomer.¹⁸

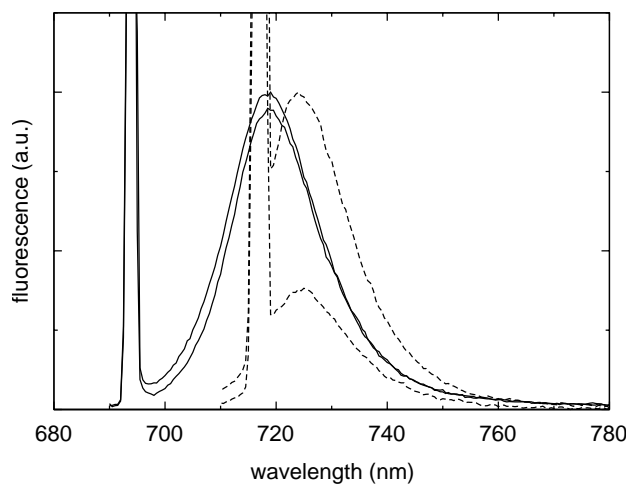
Figure 2.1 shows Soret-excited emission spectra from monomeric PSI core complexes from *Synechocystis* sp. PCC 6803 between 4 K and 120 K. The spectra are characterized by a strongly temperature-dependent contribution peaking at about 720 nm (the exact peak maxima are 720.5 nm at 77 K and at 718.5 nm at 4 K) and a small temperature-independent contribution peaking at 675.5 nm. We attribute the latter contribution to uncoupled chl absorbing at about 670 nm. The temperature-dependence of the 720 nm contribution is



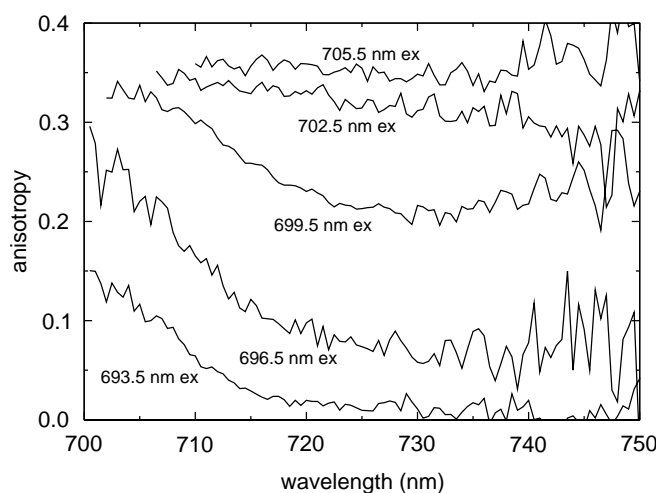
2.1 Soret excited (437 nm) emission spectra of monomeric PSI complexes from *Synechocystis* PCC 6803 at 4 K (full line, upper curve), 40 K (dashed line, upper curve), 77 K (full line, lower curve) and 120 K (dashed line, lower curve). The spectra were recorded with $A_{680} \sim 0.05$.

virtually identical to the dependence observed by Wittmershaus et al. for *Synechocystis* membranes.¹⁹

The nature of the emission at 4 K was further analysed by applying selective laser excitation in the red part of the chl $Q_{y(0-0)}$ absorption region. Figure 2.2 shows a typical result of the vertically and horizontally polarized emission spectra of monomeric complexes upon vertical excitation at 693.5 nm (continuous lines) and 716.5 nm (dashed lines). The spectra consist of sharp, high peaks at the laser excitation wavelength and broad features around



2.2 Emission spectra at 4 K of monomeric PSI complexes from *Synechocystis* PCC 6803, laser-excited at 693.5 nm (full lines) and at 716.5 nm (dashed lines). The laser excitation light was vertically polarized, and a polarizer in the detection beam selected either for vertically polarized light (upper curves) or for horizontally polarized light (lower curves). The spectra were recorded with $A_{680} \sim 1$ (see Materials and methods).

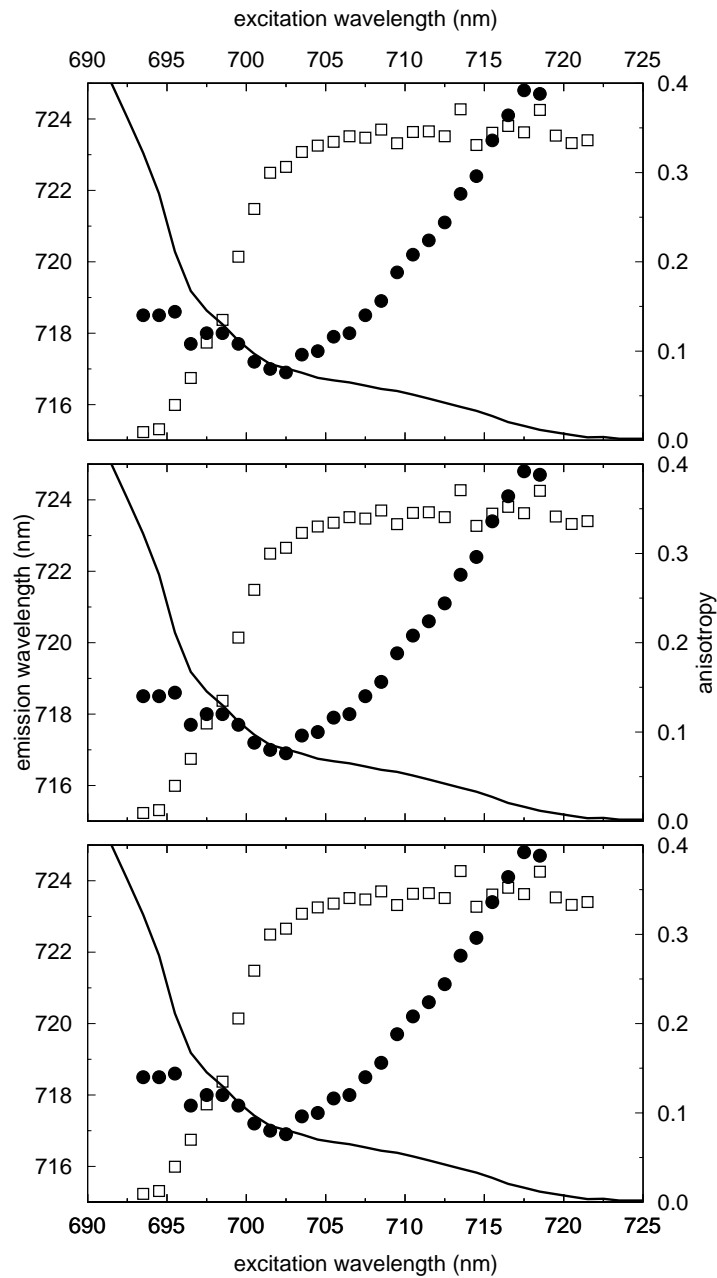


2.3 Anisotropy spectra at 4 K of monomeric PSI complexes from *Synechocystis* PCC 6803, laser-excited (from bottom-to-top) at 693.5, 696.5, 699.5, 702.5 and 705.5 nm.

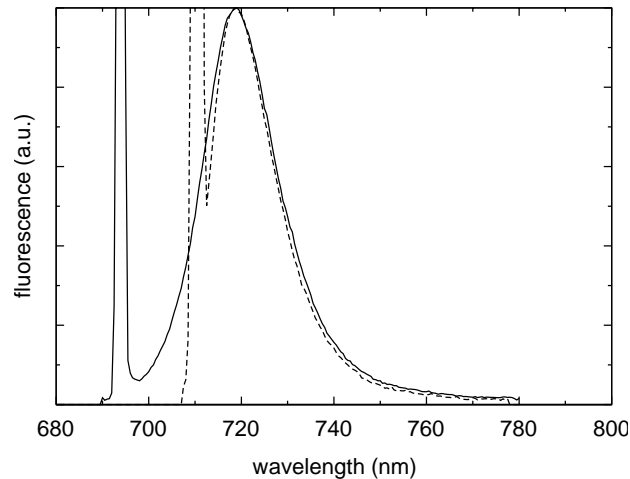
720 nm that resemble the PSI emission peaks obtained by excitation in the Soret absorption region of the chlorophylls (fig. 2.1). The contribution of uncoupled chl is not observed with both excitation wavelengths, which is expected because the excitation wavelength is well above their absorption maximum.¹⁴ The sharp features in figure 2.2 are largely due to elastic scattering of the laser excitation light. Also the contribution at the blue side of the scattering peak was found to originate from scattering, which was concluded from measurements on scattering samples without absorption at the wavelength of excitation.

It becomes immediately clear from figure 2.2 that the anisotropy of the emission depends strongly on the excitation wavelength. The vertically and horizontally detected emission spectra have about equal amplitudes upon 693.5 nm excitation, whereas they differ considerably upon 716.5 nm excitation. Figure 2.3 shows the anisotropy spectra of the emission upon selective excitation at wavelengths from 693.5 nm to 705.5 nm. At all excitation wavelengths at and above 705.5 nm the anisotropy is high (~ 0.34) and close to the theoretical maximum (0.4). This indicates that no depolarization due to energy transfer takes place at these wavelengths, although the possibility of energy transfer between pigments with almost perfectly aligned Q_y transitions cannot be ruled out. In figure 2.4a (open squares) the value of the anisotropy detected at 735 nm is plotted. It shows a steep rise from almost zero at 693.5 nm to about 0.34 above 705.5 nm and is almost identical to the fluorescence polarization spectra at 77 K.¹⁰ For excitation wavelengths between 693.5 and 705.5 nm the anisotropy of the emission depends on the detection wavelength; close to the scattering peak at the blue side of the emission band the anisotropy increases to some extent (fig. 2.3). This is not due to a contribution of polarized scattered light (anisotropy 1.0), because the region of increased anisotropy extends more to the red than the scattered light and because it is not observed upon excitation above 705.5 nm.

Another feature of the site-selected emission spectra of figure 2.2 is that the peak-wavelength of the emission depends on the excitation wavelength. The values of the emission maxima are plotted in figure 2.4a (closed circles) as a function of excitation



2.4 (A) Emission and absorption characteristics of monomeric PSI complexes from *Synechocystis* PCC 6803 at 4 K. Closed circles: wavelength of the emission maximum (λ_{em}) as a function of excitation wavelength (λ_{ex}). Open squares: value of the anisotropy of the emission detected at 735 nm. Line: 4 K absorption spectrum. (B) As A, but of trimeric PSI complexes from *Synechocystis* PCC 6803 at 4 K. (C) As A, but of thylakoid membranes from *Synechocystis* PCC 6803 at 4 K.



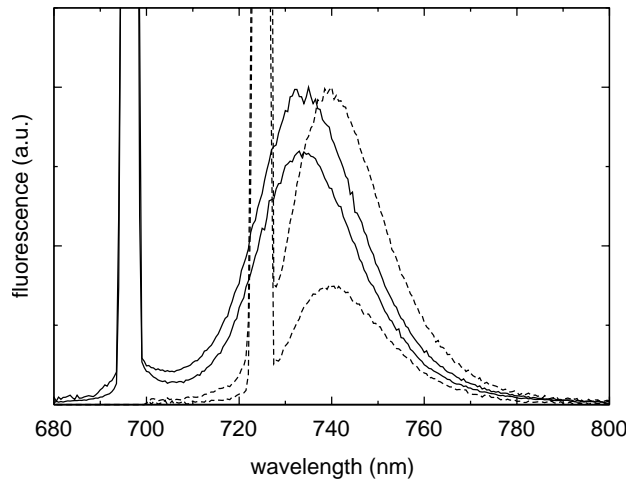
2.5 Comparison of the spectral shape of emission spectra of monomeric PSI complexes from *Synechocystis* PCC 6803 at 4 K excited at 693.5 nm (full line) and 712.5 nm (dashed line, blue-shifted by 2 nm). The spectra were normalized at the peak of the emission at 718.5 nm.

wavelength. Striking is the fact that upon red shifting the wavelength of excitation the emission maximum first blueshifts to about 717 nm upon excitation at 702 nm, and then red shifts with a slope of about 0.6. Figure 2.5 compares the shapes of the emission spectra obtained upon relatively blue (693.5 nm) and relatively red excitation (712.5 nm). The width and shape on the red side of the emission spectra are very similar, whereas the width on the blue side decreases upon far red excitation. The same phenomenon was also observed in the antenna of *Rhodospseudomonas viridis* (Monshouwer et al., unpublished observations).

Figure 2.4b and c show that site-selected fluorescence measurements on trimeric particles and thylakoid membranes from *Synechocystis* sp. PCC 6803 yield basically the same results as obtained for monomeric particles. This shows that the long-wavelength pigments that are responsible for the steady-state emission at 4 K are basically unperturbed during the isolation procedure. This also indicates that in the trimeric particles there is no excitation energy transfer among the long-wavelength pigments at 4 K (which confirms conclusions in ref. 10 at 77 K), because otherwise the anisotropy and peak wavelength of emission would show a dependence on excitation wavelength different from that observed in the monomers.

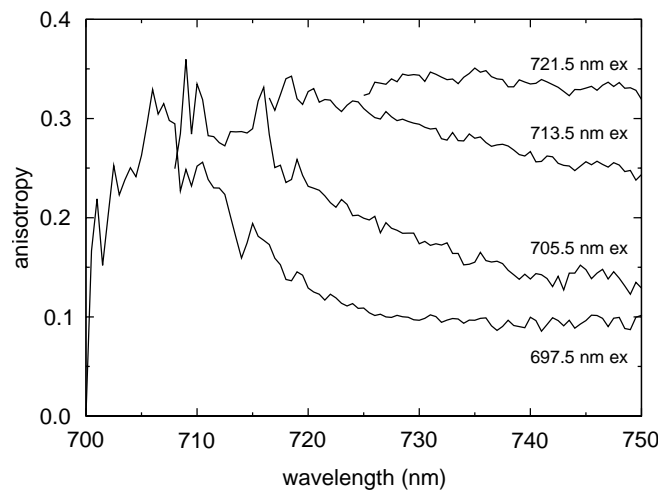
PSI-200 complexes from spinach

Polarized site-selected fluorescence experiments were also performed on PSI-200 complexes from spinach. These complexes consist of a monomeric PSI core surrounded by about 8 chl*a/b* containing LHCl proteins.²⁰ The latter proteins contain long-wavelength pigments that are responsible for steady-state fluorescence peaking at about 735 nm.⁹ These pigments absorb and fluoresce more to the red than the long-wavelength pigments of the core antenna of PSI. Van der Lee et al.¹⁰ suggested that excitations are effectively transferred from the long-wavelength pigments of the core antenna to the long-wavelength pigments of the peripheral antenna at low temperatures.

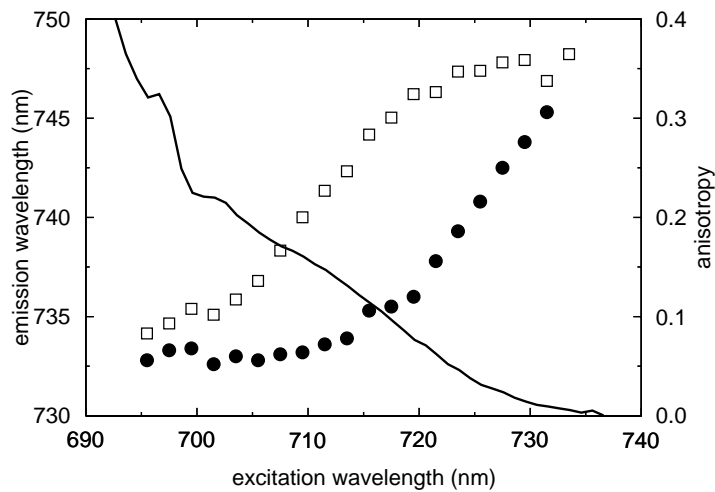


2.6 Emission spectra at 4 K of PSI-200 complexes from spinach, laser-excited at 695.5 nm (full lines) and at 723.5 nm (dashed lines). The laser excitation light was vertically polarized, and a polarizer in the detection beam selected either for vertically polarized light (upper curves) or for horizontally polarized light (lower curves). The spectra were recorded with $A_{680} \sim 1$ (see Materials and methods).

Figure 2.6 shows a typical result of polarized site-selected fluorescence experiments of PSI-200. Again, pronounced scattering peaks are observed around the excitation wavelength, as well as excitation-wavelength dependent anisotropies and peak wavelengths of the emission. The anisotropy spectra of the emission for a number of applied excitation wavelengths are shown in figure 2.7. For excitation wavelengths from 695.5 to 713.5 nm it shows a region of increased anisotropy close to the excitation wavelength, similar to excitation wavelengths below 705.5 nm in the PSI core particles from *Synechocystis*. As the excitation wavelength is shifted from the blue to the red side of this region, the red tail of the

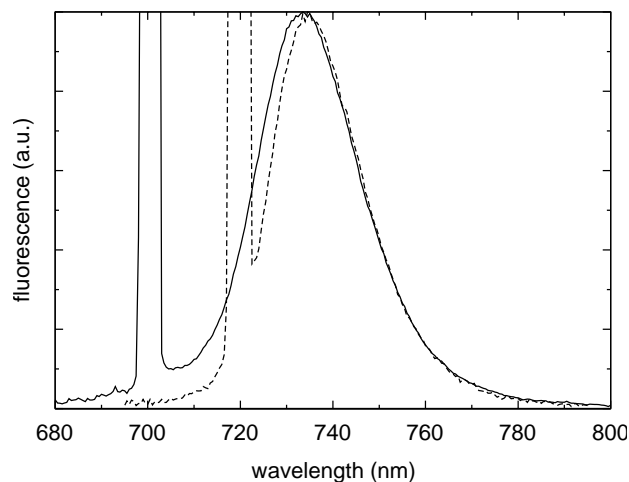


2.7 Anisotropy spectra at 4 K of PSI-200 complexes from spinach, laser-excited (from bottom-to-top) at 697.5, 705.5, 713.5 and 721.5 nm.



2.8 Emission and absorption characteristics of PSI-200 complexes from spinach at 4 K. Closed circles: wavelength of the emission maximum (λ_{em}) as a function of excitation wavelength (λ_{ex}). Open squares: value of the anisotropy of the emission detected at 750 nm. Line: 4 K absorption spectrum.

anisotropy rises until the anisotropy spectra are constant over the entire emission band. The flat, high anisotropy occurs with excitation wavelengths at and above 721.5 nm (see also figure 2.8, open squares). The peak wavelength of the emission is constant at excitation wavelengths below 715 nm (Figure 2.8, closed circles). Above 719 nm it starts to rise almost linearly upon red shifting the excitation with a slope of about 0.77. This slope is steeper than the slope observed in the PSI particles of *Synechocystis*, and a dip as in the corresponding experiments on *Synechocystis* (Figure 2.4a-c, closed circles) is not observed. Figure 2.9 compares the shapes of the emission spectra obtained upon relatively blue (699.5 nm) and



2.9 Comparison of the spectral shape of emission spectra of PSI-200 complexes from spinach at 4 K excited at 699.5 nm (full line) and 723.5 nm (dashed line, blueshifted by 5 nm). The spectra were normalized at the peak of the emission at 733.5 nm.

relatively red excitation (723.5 nm). As in *Synechocystis*, the width and shape on the red side of the emission spectra are the same, whereas the width on the blue side decreases upon far red excitation.

DISCUSSION

The polarized site-selected emission experiments of PSI reaction centre core and peripheral antenna complexes presented in this contribution show that anisotropy and peak wavelength of the emission depend on the excitation wavelength. Polarized site-selected emission experiments have also been performed on isolated LH1 antenna complexes from *Rhodobacter sphaeroides*,²¹ the B820 subunit of the LH1 antenna complex of *Rhodospirillum rubrum*,²² chl a in detergent¹⁴ and the isolated PSII reaction centre complex,²³ and results of these experiments have been explained in terms of downhill energy-transfer among a specific cluster of pigments and homogeneous and inhomogeneous broadening of spectral bands.

Inhomogeneous broadening

In general, spectral lines can be inhomogeneously and homogeneously broadened.²⁴⁻²⁶ Inhomogeneous broadening of the absorption bands (Γ_i) reflects variations in the energies of the electronic transitions of the pigments. These variations arise from slightly different conformations of the protein environment of the pigment. The various conformations will be frozen at very low temperatures, due to which pigments in those conformations can selectively be excited by steady-state laser light. Homogeneous broadening (Γ_h) is usually defined as broadening of the zero-phonon transition. Another form of broadening, which also may be regarded as a form of homogeneous broadening, stems from electron-phonon coupling, which leads to asymmetric broadening towards the high-energy side of the absorption band, reflected by a phonon side-band. The phonon side-band actually carries a significant part of the oscillator strength of the transition; it will also appear in the fluorescence spectrum but then on the low-energy side of the zero-phonon line. In the remaining part of this paper we will refer to Γ_h as the width of the phonon side-wing, since this wing is much broader than the zero-phonon line.

The site-selected emission spectra of the PSI core and peripheral antenna complexes presented in this contribution show that the optical transitions of the long-wavelength pigments responsible for the steady-state emission are considerably inhomogeneously broadened, since the shape and position of the emission spectrum depend on the excitation wavelength (see Appendix). We just note here that homogeneous broadening is also very significant for the description of the spectral properties of the long-wavelength pigments (see below).

The concept of inhomogeneous broadening has consequences for the shape of the PSI core emission spectra at intermediate temperatures (e.g., 77 K). At these temperatures there is slow uphill energy-transfer from the long-wavelength pigments to the primary electron donor P700, which forms a very efficient energy trap. The uphill transfer will be more efficient for long-wavelength pigments absorbing at the blue side of the inhomogeneous distribution than for those at the red side, due to which the red part will contribute more to the fluorescence.

The spectra presented in figure 2.1 show that indeed the emission red shifts upon raising the temperature from 4 K to 77 K, and therefore give further support to the inhomogeneous broadening of the long-wavelength pigments of PSI. This also shows that one has to be careful about assigning specific emission bands to specific pigments, because the emission spectrum may preferentially arise from a low-energy part of the inhomogeneous distribution.

Energy transfer in the PSI antenna from *Synechocystis*

The anisotropy data presented in ref. 10 and in figure 2.4 of this contribution suggest that the long-wavelength pigments in the core antenna of *Synechocystis* are either not connected by energy transfer or are connected but with almost parallel Q_y transition dipoles. However, the fact that anisotropy and peak wavelength of the emission start to rise and decrease, respectively, at the same excitation wavelength (~ 695 nm) rules out the option that parallel long-wavelength pigments are connected by energy transfer at 4 K. If two or more 'red' pigments would be coupled, the probability of energy transfer from a pigment on the blue side of the inhomogeneous distribution to another would be high, due to which the probability of emission at the blue side of the distribution would be low and the peak wavelength of emission would start to shift at a considerably longer excitation wavelength than the anisotropy (see also ref. 21).

The low anisotropy values of the emission obtained upon excitation at and below 695.5 nm are due to energy transfer from pigments which absorb below this wavelength and transfer their excitation energy to the long-wavelength pigments. Similarly, the high anisotropy values obtained upon excitation above 702 nm indicate the absence of energy transfer. Since just above 702 nm P700 should have significant absorption, it also indicates that there is no energy transfer from P700 to the long-wavelength pigments at 4 K, suggesting that P700 forms a perfect energy trap. At intermediate wavelengths a mixture of different types of pigments is excited. The resulting emission spectra revealed a relatively high anisotropy at the blue side of the emission band and a much lower anisotropy at the red side (fig. 2.3). The high anisotropy at the blue side may arise from pigments which form local energy traps and transfer the energy relatively slowly (in 10–20 ps see ref. 1) to P700 or to the long-wavelength antenna pigments.

The homogeneous bandwidth of the long-wavelength pigments in *Synechocystis*

The plot of the peak wavelength of emission versus excitation wavelength (fig. 2.4) also gives information about the relative width of the homogeneous lineshape of the long-wavelength pigments. From the anisotropy measurements it can be deduced that for excitation wavelengths above 702 nm the emission almost exclusively arises from directly excited long-wavelength pigments. The peak wavelength of the emission shifts from about 717 nm for 702 nm excitation to 725 nm for 719 nm excitation. It is remarkable that even at the latter wavelength at the far red end of the absorption spectrum the gap between excitation and peak of emission wavelength is rather high (about 6 nm, or 115 cm^{-1}). Since at this far-red excitation wavelength the pigments will be excited in their zero-phonon lines or in the red part of the phonon wing, a large proportion of this gap represents the energetic separation between the zero-phonon line and the peak of the corresponding phonon wing.

Also the spectrum obtained upon far-red excitation has a quite considerable width (see, for instance, the 716.5 nm excited spectra in figure 2.2, which are characterized by a fwhm of about 16 nm or 310 cm^{-1}).

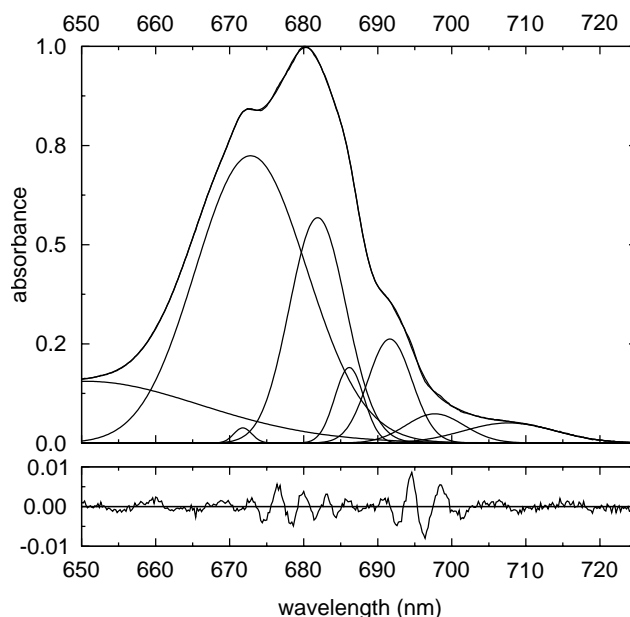
Excitation at 708 nm yielded an emission maximum at 718.5 nm. The same maximum is observed upon non-selective excitation, which suggests that the peak position of the complete absorption band of all longwavelength pigments is near 708 nm (see Appendix: $\lambda_{\text{em}} = \lambda_{0,\text{em}}$ at 718.5 nm, due to which $\lambda_0 = \lambda_{\text{ex}} = 708\text{ nm}$). We will therefore designate from now on the long-wavelength pigments of *Synechocystis* as C708.

From the slope of the λ_{em} vs. λ_{ex} plot estimates for the homogeneous (Γ_h) and inhomogeneous (Γ_i) bandwidths can be obtained (see Appendix). The slope is not very large ($s = 0.6$) and suggests $\Gamma_h/\Gamma_i \sim 0.8$. This means that C708 is characterized by a quite considerable homogeneous bandwidth. From the Gaussian fit of figure 2.10 (discussed in detail below) a value of $\sim 270\text{ cm}^{-1}$ is estimated for the total fwhm of C708 in absorption. Assuming Gaussian profiles for homogeneous and inhomogeneous broadening, this leads to values of ~ 170 and 215 cm^{-1} for Γ_h and Γ_i , respectively. The energetic separation between the peak wavelengths of absorption and emission is about 10 nm (or 200 cm^{-1}) for the total long-wavelength band, which largely represents the energetic separation between peak wavelengths of the phonon side bands in absorption and emission, i.e. the Stokes' shift δ . The difference in shape of the emission spectra upon relatively blue and red excitation (fig. 2.5) is attributed to the preferential excitation in the blue and red parts of the phonon wing, respectively.

The Stokes' shift of C708 appears much larger than of isolated chl a ($\sim 80\text{ cm}^{-1}$ - ref. 14). In principle, this large value could be due to specific interactions between the protein environment (e.g., charged amino acids) and monomeric chl a . However, we are not aware of any documented precedents. Alternatively, the large Stokes' shift of C708 may be caused by strong pigment-pigment interactions. An increased Stokes' shift was observed in the B820 subunit of the LH1 antenna of *Rhodospirillum rubrum* (about 120 cm^{-1} - ref. 27) and attributed to the dimeric nature of the Bchls. Also for the primary electron donor of the reaction centre of purple bacteria a large separation between zero-phonon line and peak wavelength of the phonon side band ($\sim 120\text{ cm}^{-1}$) was observed,²⁵ which predicts a Stokes' shift of about 240 cm^{-1} . Based on these results we propose that pigment-pigment interactions rather than pigment-protein interactions cause the large Stokes' shift of C708 and that C708 is a dimer of (excitonically coupled) chl a molecules (see also below). The CD is less than that of P700,¹⁰ which suggests that the electronic transition dipole moments of the individual molecules are more in one plane than those of P700. The transition dipole moment of the major exciton component of C708 was reported to make an angle between 17° and 28° with the plane of the particle.¹⁰

The number of long-wavelength pigments in *Synechocystis*

In our earlier report¹⁰ we mentioned that it was not possible to estimate the number of long-wavelength pigments per reaction centre by fitting the absorption spectra with Gaussian bands. Several good fits could be obtained in which peak wavelength and amplitude of the long-wavelength pigments varied quite considerably. The more accurate estimation of the peak wavelength of C708 in this contribution permits a better estimation of the oscillator



2.10 Fit with Gaussian bands of the absorption spectrum between 650 and 725 of monomeric PSI complexes from *Synechocystis* PCC 6803 at 4 K. The lower represents the (enlarged) difference between absorption spectrum and fit. Constraints: 8 Gaussians, each characterized by a certain peak wavelength (λ), FWHM and amplitude (a); all parameters were free fitting parameters. Result: band 1 (C708): $\lambda = 708.1$ nm, $fwhm = 13.5$ nm, $a = 0.049$; band 2 (P700): $\lambda = 697.9$ nm, $fwhm = 9.5$ nm, $a = 0.076$; band 3: $\lambda = 691.6$ nm, $fwhm = 7.0$ nm, $a = 0.262$; band 4: $\lambda = 686.1$ nm, $fwhm = 4.6$ nm, $a = 0.190$; band 5: $\lambda = 681.9$ nm, $fwhm = 9.0$ nm, $a = 0.567$; band 6: $\lambda = 672.8$ nm, $fwhm = 17.7$ nm, $a = 0.812$; band 7: $\lambda = 671.8$ nm, $fwhm = 2.9$ nm, $a = 0.007$; band 8: $\lambda = 650.6$ nm, $fwhm = 36$ nm, $a = 0.154$. The last band approximates a collection of vibrational bands of all spectral bands and is not included in the estimation of the oscillator strength in bands 1 and 2.

strength of C708. Figure 2.10 shows a fit with Gaussian bands of the 4 K absorbance spectrum of monomeric complexes. The result is a 13.5 nm broad Gaussian with an oscillator strength of 1.85 per 65 chls, suggesting one C708 dimer per monomeric reaction centre complex. The intensity of the P700 band at 698 nm was 2.05 per 65 chls, in agreement with its dimeric nature. We do not wish to attribute much significance to the remaining part of the fit. The fit is consistent, however, with the wavelength dependent behaviour of the anisotropy. Below 695 nm C708 has no absorption. Therefore, upon excitation below 695 nm almost all fluorescence arises after excitation energy transfer. On the other hand, the 'blue' antenna pigments do not absorb above 701 nm and excitation above 701 nm leads to highly polarized fluorescence from directly excited pigments, in agreement with the results presented in figure 2.4. The data suggest that the PSI core antenna does not contain a separate pool of antenna pigments that absorbs between C708 and the pool absorbing at 693 nm, and that C708 in *Synechocystis* may be regarded as a $N=1$ system.

Comparison with results from spectral hole-burning

It is worthwhile to compare our site-selected fluorescence data on PSI core particles with the hole-burning data by Small and co-workers.²⁸ These authors analysed PSI core particles from

spinach, which showed an absorption maximum at considerably shorter wavelength than our particles (~670 nm vs. 679 nm), but nevertheless are characterized by rather similar absorption profiles in the far red absorption region (compare, e.g., figure 2 from ref. 28 with figure 2.4 from this contribution). The hole-burning profiles were analysed in absorption, which means that (depending on the burning efficiencies) P700 and C708 may both contribute to the spectra and that the presented spectral parameters could arise from a mixture of both species. However, the presence of long-wavelength antenna pigments was not considered in ref. 28.

The hole-burning profiles obtained after irradiation at 702.6, 706.3 and 715.0 nm could reasonably well be described by a Huang-Rhys factor S of 4-6 and a mean phonon frequency ω_m of 35-50 cm^{-1} .²⁸ Because according to our fits (fig. 2.10) P700 will primarily be excited at 702.6 nm and C708 at 715 nm, we conclude that the spectral properties of both species do not differ very much. This suggests that the broad homogeneous linewidth of C708 observed in the present study is mainly caused by a large value of S , i.e., by a considerable reorganization of C708 in the excited state.

The product $S\omega_m$ approximately represents the energetic separation between the zero-phonon line and the peak of the phonon side-band.²⁵ This product was estimated by Gillie et al.²⁸ to be $\sim 200 \text{ cm}^{-1}$, which is about twice as large as estimated from our site-selected fluorescence data. We do not have an appropriate explanation for this discrepancy. Nevertheless, both values are much larger than the value of $S\omega_m \sim 20 \text{ cm}^{-1}$ obtained after burning in the 'normal' antenna at 680.5 nm.²⁸ This emphasizes the different nature of the long-wavelength antenna pigments as opposed to normal antenna pigments.

Long-wavelength antenna pigments in PSI-200 from spinach

The situation in the core/peripheral antenna of PSI-200 is more complex than in the core antenna of *Synechocystis*. There are several pools of long-wavelength antenna pigments, and because the anisotropy starts to rise at a considerably longer wavelength than in the core antenna of *Synechocystis* and in isolated LHCl,²⁹ it is clear that at least some of these pools are connected by energy transfer. Excitation wavelengths longer than about 720 nm have to be applied in order to minimize the energy transfer.

The non-selectively excited steady-state emission spectrum is characterized by a broader bandwidth (FWHM $\sim 470 \text{ cm}^{-1}$ vs. $\sim 340 \text{ cm}^{-1}$ for *Synechocystis*). Because the slope of the λ_{em} vs. λ_{ex} plot is steeper (~ 0.77 in PSI-200 vs. ~ 0.6 in *Synechocystis*) we suggest that an increase of the inhomogeneous bandwidth is primarily responsible for the increased emission bandwidth of the red-most pool of long-wavelength pigments in PSI-200. According to calculations as in the Appendix, we estimate $\Gamma_h/\Gamma_i \sim 0.55$. With a somewhat higher value for Γ_h as in *Synechocystis* (200 cm^{-1}) and a 1/0.55 higher value for Γ_i ($\sim 360 \text{ cm}^{-1}$), the total bandwidth in absorption will be $\sim 400 \text{ cm}^{-1}$, which seems a reasonable value.

The energetic separation between the zero-phonon line and the peak of the phonon wing (i.e. the value of $S\omega_m$) should be relatively large in PSI-200, since excitation at the far red end of the absorption spectrum (732 nm) still yielded a shift of 13 nm (240 cm^{-1}), which is about twice as large as in the core antenna of *Synechocystis*. Thus, the shape of the emission spectra upon far red excitation differs considerably for the two analysed systems: the value of $S\omega_m/\Gamma_h$ is about 0.57 in *Synechocystis* and 1.0 in PSI-200. Because the value of $S\omega_m$ is even larger in

PSI-200 than in *Synechocystis*, we propose, in line with the discussions described above for *Synechocystis*, that pigment-pigment interactions also determine the spectroscopic properties of the red-most long-wavelength pigments in PSI-200.

The data also permit an estimation of the peak wavelength of the total absorption band of the longwavelength pigments. Substituting values from the λ_{em} vs. λ_{ex} plot (for the region $\lambda_{ex} > 720$ nm - see figure 2.8) into equation 2-8 yields $\lambda_0 = 716$ nm. This value is somewhat less accurate than that of C708, because it is uncertain in which extent the long-wavelength pigments are connected by energy transfer. Introduction of energy transfer would shift the peak wavelength of the long-wavelength pigments to shorter wavelengths.²¹ A Stokes' shift δ of 17 nm, however, seems reasonable in view of the parameters described above. Therefore, we propose to denote the long-wavelength pigments in the peripheral antenna of PSI as C716.

ACKNOWLEDGEMENTS

This research was supported in part by the Netherlands Foundations for Chemical Research (SON) and for Biophysics (SvB), financed by the Netherlands Organization for Scientific Research (NWO). J.P.D. was supported by a fellowship from the Royal Academy of Arts and Sciences (KNAW). J.K. and M.R. were supported by a grant from the Deutsche Forschungsgesellschaft (DFG).

APPENDIX

In this appendix the fluorescence behaviour of a pool of non-transferring pigments upon site selected excitation is described. The position of the fluorescence maximum λ_{em} for excitation at a particular wavelength λ_{ex} depends on the relative contributions of homogeneous and inhomogeneous broadening to the absorption spectrum. In order to illustrate this we first consider two extreme cases:

- 1 The homogeneous broadening is negligible with respect to the inhomogeneous broadening. This is for instance the case when the absorption spectrum is solely determined by the zero-phonon line and the phonon sideband is absent. In that case both absorption and emission occur through the same zero-phonon transition and $\lambda_{em} = \lambda_{ex}$. This leads to a maximum value for the slope s defined as $d(\lambda_{em})/d(\lambda_{ex})$, namely $s=1$;
- 2 The inhomogeneous broadening is negligible with respect to the homogeneous broadening. In that case λ_{em} does not depend on λ_{ex} and $s = 0$. For pigments in a protein environment both types of broadening are significant and this leads to values of s between 0 and 1.

We consider now the case of individual pigments which do not transfer energy to each other. All pigments are assumed to have identically shaped absorption and emission spectra and the difference δ between the absorption and emission maxima (Stokes' shift) is also assumed to be identical. In all cases a wavelength scale is used. A frequency (energy) scale would be more appropriate but is not necessary at the current level of approximation. The maxima of the

absorption spectra of individual pigments are distributed according to a distribution function $IDF(\lambda)$, which is usually taken to be Gaussian:³⁰

$$IDF(\lambda) = \frac{1}{\sqrt{\pi}\sigma_i} e^{-(\lambda - \lambda_0)^2 / \sigma_i^2} \quad 2-1$$

Here λ_0 denotes the centre of the distribution and σ_i is proportional to the inhomogeneous width Γ_i (FWHM) of the distribution according to $\Gamma_i = 1.67\sigma_i$. At first, the zero-phonon line will be omitted. Its effect will be discussed later. Therefore, the absorption spectrum is fully determined by the phonon sideband. Its shape is chosen to be Gaussian (see also below), since this allows an easy mathematical treatment. For a single chromophore with its absorption maximum at λ , the absorption at a particular wavelength of excitation λ_{ex} is given by:

$$\varepsilon_\lambda(\lambda_{ex}) = \frac{1}{\sqrt{\pi}\sigma_h} e^{-(\lambda - \lambda_{ex})^2 / \sigma_h^2} \quad 2-2$$

σ_h is proportional to the width of the homogeneous broadening Γ_h (FWHM) according to $\Gamma_h = 1.67\sigma_h$. Note that the maximum of the total absorption spectrum is at λ_0 . The maximum of the total fluorescence spectrum $\lambda_{0,em}$ (which can be obtained upon non-selective excitation, e.g. in the Soret region) is then at $\lambda_{0,em} = \lambda_0 + \delta$.

The number of pigments $N(\lambda)$ with an absorption maximum at λ , excited by excitation light with wavelength λ_{ex} , is proportional to $P(\lambda)$ which is defined as

$$P(\lambda) = IDF(\lambda)\varepsilon_\lambda(\lambda_{ex}) \quad 2-3$$

and substitution of equations 2-1 and 2-2 into equation 2-3 leads to

$$P(\lambda) = \frac{1}{\pi\sigma_i\sigma_h} e^{\{-(\lambda - \lambda_0)^2 / \sigma_i^2 - (\lambda - \lambda_{ex})^2 / \sigma_h^2\}} \quad 2-4$$

$P(\lambda)$ also has a Gaussian shape with a maximum at $\lambda_0 + \{\sigma_i^2 / (\sigma_i^2 + \sigma_h^2)\}(\lambda_{ex} - \lambda_0)$. The wavelength $\lambda_{abs-max}$ where $N(\lambda)$ is largest is thus $\lambda_0 + \{\sigma_i^2 / (\sigma_i^2 + \sigma_h^2)\}(\lambda_{ex} - \lambda_0)$ and the maximum of the fluorescence spectrum (λ_{em}) is at $\lambda_{abs-max} + \delta$. This leads to:

$$\lambda_{em} = \lambda_0 + \delta + \frac{\sigma_i^2}{\sigma_i^2 + \sigma_h^2}(\lambda_{ex} - \lambda_0) \quad 2-5$$

Therefore,

$$s = \frac{d(\lambda_{em})}{d(\lambda_{ex})} = \frac{\sigma_i^2}{\sigma_i^2 + \sigma_h^2} \quad 2-6$$

and

$$\lambda_{em} = \lambda_0 + \delta + s(\lambda_{ex} - \lambda_0) = \lambda_{0,em} + s(\lambda_{ex} - \lambda_0) \quad 2-7$$

Note that $\sigma_i^2/(\sigma_i^2 + \sigma_h^2) = \Gamma_i^2/(\Gamma_i^2 + \Gamma_h^2) = \Gamma_i^2/\Gamma_{tot}^2$ where Γ_{tot} is the FWHM of the entire absorption band, caused by both homogeneous and inhomogeneous broadening.

From equation 2-7 the maximum λ_0 of the total absorption band and the Stokes' shift δ can be determined according to:

$$\lambda_0 = \lambda_{ex} - (1/s)(\lambda_{em} - \lambda_{0,em}) \quad 2-8$$

$$\delta = \lambda_{0,em} - \lambda_0 \quad 2-9$$

Clearly, these relations hold in the linear region of s . In the case of the red pigments in PSI, the contribution of the zero-phonon line is negligible (see Discussion and ref. 29) and the absorption spectrum is mainly determined by the phonon sideband. Although a Gaussian shape of this sideband is not realistic, this particular choice will not significantly influence the conclusions very much near the centre of the total absorption band. For instance, a Lorentzian shape will give very similar results as long as the extreme wings of the absorption spectrum are not taken into account (calculations not shown). Finally, we note that in case the contribution of the zero-phonon line is not negligible it will lead to an increase of s , since for very small homogeneous bandwidths (like that of the zero-phonon line) the slope $s=1$.

REFERENCES

- (1) Van Grondelle, R., J.P. Dekker, T. Gillbro, and V. Sundström. 1994. Energy-transfer and trapping in photosynthesis. *Biochim. Biophys. Acta.* 1187:1-65.
- (2) Lin, S., H. van Amerongen, and W.S. Struve. 1992. Ultrafast pump-probe spectroscopy of the P700-containing and F_x -containing Photosystem-I core protein from *Synechococcus* sp. PCC-6301 (*anacystis-nidulans*). *Biochim. Biophys. Acta.* 1140:6-14.
- (3) Du, M., X. Xie, Y. Jia, L. Mets, and G.R. Fleming. 1993. Direct observation of ultrafast energy-transfer in PSI core antenna. *Chem. Phys. Lett.* 201:535-542.
- (4) Werst, M., Y. Jia, L. Mets, and G.R. Fleming. 1992. Energy-transfer and trapping in the Photosystem-I core antenna - a temperature study. *Biophys. J.* 61:868-878.
- (5) Holzwarth, A.R., G. Schatz, H. Brock, and E. Bittersman. 1993. Energy-transfer and charge separation kinetics in Photosystem-I. 1. Picosecond transient absorption and fluorescence study of cyanobacterial Photosystem-I particles. *Biophys. J.* 64:1813-1826.

- (6) Trissl, H.-W. 1993. Long-wavelength absorbing antenna pigments and heterogeneous absorption-bands concentrate excitons and increase absorption cross-section. *Photosynth. Res.* 35:247-263.
- (7) Trissl, H.-W., and C. Wilhelm. 1993. Why do thylakoid membranes from higher-plants form grana stacks? *Trends Biochem. Sci.* 18:415-419.
- (8) Van Grondelle, R., H. Bergström, V. Sundström, R.J. van Dorssen, M. Vos, and C.N. Hunter. 1988. *In Photosynthetic LightHarvesting Systems*. H. Scheer, and S. Schneider, editors. Walter de Gruyter, Berlin. 519-530.
- (9) Holzwarth, A.R. 1991. Excited-state kinetics in chlorophyll systems and its relationship to the functional organization of the photosystems. *In Chlorophylls*. H. Scheer, editor. CRC Press, Boca Raton, FL. 1125-1151.
- (10) Van der Lee, J., D. Bald, S.L.S. Kwa, R. van Grondelle, M. Rögner, and J.P. Dekker. 1993. Steady-state polarized-light spectroscopy of isolated Photosystem-I complexes. *Photosynth. Res.* 35:311-321.
- (11) Rögner, M., P. Nixon, and B.A. Diner. 1990. Purification and characterization of Photosystem-I and Photosystem-II core complexes from wild-type and phycocyanin-deficient strains of the cyanobacterium *Synechocystis* PCC-6803. *J. Biol. Chem.* 265:6189-6196.
- (12) Kruij, J., E.J. Boekema, D. Bald, A.F. Boonstra, and M. Rögner. 1993. Isolation and structural characterization of monomeric and trimeric Photosystem-I complexes (P700:F_a/F_b and P700:F_x) from the cyanobacterium *Synechocystis* PCC-6803. *J. Biol. Chem.* 268:23353-23360.
- (13) Kwa, S.L.S., W.R. Newell, R. van Grondelle, and J.P. Dekker. 1992. The reaction center of Photosystem-II studied with polarized fluorescence spectroscopy. *Biochim. Biophys. Acta.* 1099:193-202.
- (14) Kwa, S.L.S., S. Völker, N.T. Tilly, R. van Grondelle, and J.P. Dekker. 1994. Polarized site-selection spectroscopy of chlorophyll-*a* in detergent. *Photochem. Photobiol.* 59:219-228.
- (15) Boekema, E.J., J.P. Dekker, M. van Heel, M. Rögner, W. Saenger, I. Witt, and H.T. Witt. 1987. Evidence for a trimeric organization of the Photosystem I complex from the thermophilic cyanobacterium *Synechococcus* sp. *FEBS Lett.* 217:283-286.
- (16) Hladik, J., and D. Sofrová. 1991. Does the trimeric form of the Photosystem-I reaction center of cyanobacteria *in vivo* exist? *Photosynth. Res.* 29:171-175.
- (17) Chitnis, V.P., and P.R. Chitnis. 1993. PsaL subunit is required for the formation of Photosystem-I trimers in the cyanobacterium *Synechocystis* sp. PCC-6803. *FEBS Lett.* 336:330-334.
- (18) Kruij, J., D. Bald, E.J. Boekema, and M. Rögner. 1994. Evidence for the existence of trimeric and monomeric Photosystem-I complexes in thylakoid membranes from cyanobacteria. *Photosynth. Res.* 40:279-286.
- (19) Wittmershaus, B.P., V.M. Woolf, and W.F.J. Vermaas. 1992. Temperature-dependence and polarization of fluorescence from Photosystem-I in the cyanobacterium *Synechocystis* sp. PCC-6803. *Photosynth. Res.* 31:75-87.
- (20) Boekema, E.J., R.M. Wynn, and R. Malkin. 1990. The structure of spinach Photosystem-I studied by electron-microscopy. *Biochim. Biophys. Acta.* 1017:49-56.
- (21) Van Mourik, F., R.W. Visschers, and R. van Grondelle. 1992. Energy-transfer and aggregate size effects in the inhomogeneously broadened core light-harvesting complex of *Rhodobacter-sphaeroides*. *Chem. Phys. Lett.* 193:1-7.
- (22) Visschers, R.W., F. van Mourik, R. Monshouwer, and R. van Grondelle. 1993. Inhomogeneous spectral broadening of the B820 subunit form of LH1. *Biochim. Biophys. Acta.* 1141:238-244.

-
- (23) Kwa, S.L.S., N.T. Tilly, C. Eijkelhoff, R. van Grondelle, and J.P. Dekker. 1994. Site-selection spectroscopy of the reaction-center complex of Photosystem-II. 2. Identification of the fluorescing species at 4 K. *J. Phys. Chem.* 98:7712-7716.
- (24) Völker, S. 1989. Hole-burning spectroscopy. *Annu. Rev. Phys. Chem.* 40:499-530.
- (25) Reddy, N.R.S., P.A. Lyle, and G.J. Small. 1992. Applications of spectral hole burning spectroscopies to antenna and reaction center complexes. *Photosynth. Res.* 31:167-194.
- (26) Avarmaa, R.A., and K.K. Rebane. 1985. High-resolution optical spectra of chlorophyll molecules. *Spectrochim. Acta.* 41A:1365-1380.
- (27) Pullerits, T., F. van Mourik, R. Monshouwer, R.W. Visschers, and R. van Grondelle. 1994. Electron-phonon coupling in the B820 subunit form of LH1 studied by temperature-dependence of optical-spectra. *J. Luminescence.* 58:168-171.
- (28) Gillie, J.K., P.A. Lyle, G.J. Small, and J.H. Golbeck. 1989. Spectral hole burning of the primary electron-donor state of Photosystem-I. *Photosynth. Res.* 22:233-246.
- (29) Mukerji, I., and K. Sauer. 1990. Optical spectroscopy on a Photosystem I antenna complex. *In* Current research in photosynthesis. M. Baltscheffsky, editor. Kluwer, Dordrecht, the Netherlands. 2:321-324.
- (30) Jankowiak, R., and G.J. Small. 1993. Spectral Hole Burning: A window on excited state electronic structure, heterogeneity, electron-phonon coupling and transport dynamics of photosynthetic units. *In* The photosynthetic reaction center. J. Deisenhofer, and J. Norris, editors. Academic Press, New York. 2:133-176.

